Research article

X-RAY Spectrometry

Received: 2 May 2011 Revised: 13 September 2011 Accepted: 21 September 2011 Published online in Wiley Online Library

(wileyonlinelibrary.com) DOI 10.1002/xrs.1369

Evaluation of the utility of handheld XRF in meteoritics

Florian J. Zurfluh,[a]* Beda A. Hofmann,[b] Edwin Gnos[c] and Urs Eggenberger[a]

We tested a handheld X-ray fluorescence instrument with adaptable matrix correction for its suitability in meteoritics. We report here the instrument setup, precision and accuracy and present examples of applications. With a measuring time of 300 s, it is possible to collect accurate data for K, Ca, Ti, Cr, Mn, Fe, Co, Ni, Sr and Ba that are needed for the identification of doubtful meteorites and the nondestructive classification of chondrites and achondrites. The factory-supplied calibration curve of the instrument was fine tuned for our purposes with the use of well-analyzed meteorite powders, pressed pellets and meteorite hand specimens as standards. Relative errors of 10% to 20% are reached for the mentioned elements. The instrument was tested in the hot desert of Oman while searching for meteorites and also in the laboratory while doing research on meteorites. The main applications of the instrument are the identification and classification of meteorites, the quantification of terrestrial elemental contamination (Sr and Ba) and detection of Mn-rich desert varnish. It is possible to discriminate the major meteorite groups using Fe/Mn and Ni values. Handheld X-ray fluorescence is also useful in identifying meteorites belonging to the same fall event. Copyright © 2011 John Wiley & Sons, Ltd.

Keywords: handheld XRF; meteorite; terrestrial contamination; bulk composition; classification

Introduction

The determination of bulk chemical composition is essential for the identification and classification of rocks. Since nearly half of a century, X-ray fluorescence (XRF) has been used as a standard analytical method in the Earth sciences. The advantages of XRF, i.e. speed and nondestructive, were recognized early in meteoritics.[1] Whereas, typically, X-ray tubes are used to provide excitation X-rays, early portable instruments used radioactive sources instead, thus having the disadvantages of safety problems and an unavoidable degradation of the source activity over time. In the last 10 years, the availability of miniature X-ray tubes has allowed the development of field portable XRF devices, and a number of instruments are now commercially available. Handheld XRF (HHXRF, the most popular; also known as field portable XRF or portable XRF) instruments are now widely used by the industry, academia and government agencies. Prominent applications are the determination of heavy metal elements at contaminated sites, ore exploration, investigation of archeological artifacts, determination of pigments in paints and, by far the most popular of them, analysis of metals and alloys (e.g. Goldstein *et al*.,[2] Radu and Diamond,[3] Roldan *et al*.,[4] Szokefalvi-Nagy *et al*.,[5] Bonizzoni *et al*.,[6] and Huo *et al*.,[7]). Reasons for the success of HHXRF are its easy handling, speed of analysis, and portability. Another important factor, especially in dealing with rare samples, is the possibility to perform nondestructive, reproducible analyses.

Meteorites are rock fragments fallen to the surface of solar system bodies (for a definition of the term meteorite, see Rubin and Grossman;[8] for general information, e.g. see Norton and Chitwood[9]). Most commonly, meteorites are derived from the asteroid belt. In some rare instances, meteorites from Mars and the Moon reach Earth. All these extraterrestrial materials are of high potential value for science, as they provide the vast majority of information about bodies in our solar system. This work was performed as part of a meteorite search and research project in collaboration with the Ministry of Commerce, Sultanate of Oman. Our institution has a long-term partnership with Oman. In the frame of this project, meteorites are searched, documented and collected in the hot desert of Oman and classified and investigated in laboratories mainly in Switzerland.

Notwithstanding the large number of meteorites found in cold (e.g. Antarctica[10]) and hot deserts (e.g. Australia,[11–13] Sahara,[14–17] Arabia,[18,19] Atacama[20] and the USA[21,22]), these space rocks remain unique, rare and precious samples helping us to understand the early evolution of the Solar system. Because we have to take care of these valuable samples, fast and nondestructive methods for determination of meteorite types are needed. One such method is the measurement of the magnetic susceptibility.[23–25] Although very powerful for meteorites with a low degree of alteration, this method is unreliable when terrestrial weathering changes the magnetic signal.

The aims of our study were to test the suitability of HHXRF in terms of analytical precision and accuracy and to demonstrate its usefulness in several branches of meteoritics, including meteorite identification and classification, and the quantification of terrestrial elemental contamination. We tested the instrument as an 'average user' without the ability to influence the internal data processing procedure. We show that identification and

* *Correspondence to: Florian J. Zurfluh, Institute of Geological Sciences, Baltzerstrasse 1 + 3, CH-3012 Bern, Switzerland.*
E-mail: florian.zurfluh@geo.unibe.ch

a *Institute of Geological Sciences, Baltzerstrasse 1 + 3, CH-3012 Bern, Switzerland*

b *Naturhistorisches Museum der Burgergemeinde Bern, Bernastrasse 15, CH-3005 Bern, Switzerland*

c *Muséum d'histoire naturelle de la Ville de Genève, 1 Route de Malagnou, CH-1211 Genève 6, Switzerland*

classification of many common meteorite types based on element ratios (Fe/Mn) and bulk concentrations (Ni, Ca, K and Ti) are possible, whereas Ba and Sr are the most important elemental indicators of terrestrial weathering and contamination. Here, we present our findings obtained with the best optimized calibration setup.

Methods

The instrument

The instrument used for this study is a NITON XL3t-600 (Thermo Fisher Scientific, Billerica, MA, USA) energy-dispersive XRF analyzer calibrated for geological samples. It is equipped with a miniature X-ray tube with an Au anode (maximum 50 kV, 2 W and 40 μA) and three primary beam filters to provide optimized excitation energies for different elements (Table 1).[26] Their task is to reduce spectral background under analytes lines and selectively filter primary beam of X-rays from the tube. The instrument that we have used in this study was equipped with silicon p-i-n diode detector (PIN) with typical energy resolution better than 200 eV. The latest (2011) version of the analyzer is equipped with silicon drift detector (SDD), which can sustain much higher count rates and offers better energy resolution (typically 175 eV). The diameter of measured area on sample is about 8 mm, but it can be reduced to 3 mm using built-in small spot collimator. Normally, the measurements are performed using the 8-mm spot. The small spot collimator is sparsely used, e.g to measure inclusions or larger grains. A build in camera helps to fix the position. The detector operating temperature is thermoelectrically stabilized with a Peltier element to −25 °C. The detector signal is processed by a central processing unit and stored in the form of an X-ray spectrum with 4000 channels corresponding to 60 keV. The spectra of the measurements are overlaid on a computer using Niton data transfer software. During a single analysis, data are sequentially collected, first using the 'main filter' (excitation 40 kV, 50 μA, material: Al/Fe), followed by the 'low filter' (20 kV, 100 μA, Cu) and the 'high filter' (50 kV, 40 μA, Mo) (Table 1). Counting times of each filter are adjustable. Table 1 lists the elements for which the instrument was delivered with factory calibrations for ambient conditions, i.e. without He gas flushing. About 30 elements ranging from S to U are detectable, but some of them usually are below the limit of detection (LOD) in typical geological samples. It is possible to flush the chamber between the sample and the detector with helium gas for the analysis of low-energy characteristic X-rays of Mg, Al, Si and P. The latest generations of HHXRF devices that are currently on the market have SDD and are able to detect these light elements also under ambient (w/o He flush) conditions.

Two measuring modes are available: 'Soil' mode and 'Mining' mode. The main difference between these two modes is the type of algorithms used for quantifying the elements. 'Soil' mode uses the element-to-Compton peak ratio method in which the intensity of the region of interest (ROI) of a given element is divided by the intensity of the Compton peak, and then, quantification is calculated using a calibration curve. ROI is an integral of spectrum between two boundary channels (energies). At low concentrations, the X-ray intensities of the analytes and the intensity of Compton scattered X-rays are mainly affected by their absorption in the sample. Therefore, the rationing analyte intensity (ROI) to Compton peak intensity linearizes the calibration curve for that analyte. For this reason, the 'Soil' mode is preferred for quantifying heavy metal contamination in soils where contaminants typically are present at low concentration levels. However, when analyzing ores and minerals, we are faced with very large variations in composition of samples, which are the

Table 1. List of element lines measured with the three filters at different X-ray tube energies

Soil mode	Mining mode	Measuring time
Main, 40 kV, 50 μA		F[c]: 30 s; L[d]: 120 s
	Ag	
As	As	
	Bal[b]	
	Bi	
	Cd	
Co	Co	
Cu	Cu	
Fe	Fe	
	Hf	
Hg[a]		
Mn	Mn	
Mo	Mo	
	Nb	
Ni	Ni	
Pb	Pb	
	Pd	
Rb	*Rb*	
	Re	
	Sb	
Se	*Se*	
	Sn	
Sr	Sr	
	Ta	
	Ti	
Th		
U		
	V	
W	*W*	
Zn	Zn	
Zr	Zr	
Low, 20 kV, 100 μA		F: 30 s L: 60 S
Ca	Ca	
Cr	Cr	
K	K	
S	S	
Sc		
Ti	Ti	
V	V	
High, 50 kV, 40 μA		F: 0 s; L 120 s
Ag	*Ag*	
Ba	Ba	
Cd	Cd	
Cs		
Pd	Pd	
Sb	Sb	
Sn	Sn	
Te		

[a]Italic: usually bellow detection limit.
[b]Bal: 'balance', virtual element for balance.
[c]F: field.
[d]L: laboratory.

source of severe absorption and enhancement effects and which cannot be corrected by the element-to-Compton ratio method. In such a situation, the 'Mining' mode based on a fundamental parameter (FP) approach is effective. FPs-based algorithms account for all matrix effects taking place in analyzed materials because they are nonlinear, transcendental equations; they are solved numerically by iteration. The intensity of the Compton backscattered radiation is used to represent the sum of all elements that are not measured directly via their characteristic X-rays (such as oxygen, nitrogen etc.) but which contribute to the intensity of the Compton scattered radiation. We exclusively used the 'Mining' mode for this study because preliminary tests showed it to be more robust and more accurate than the 'Soil' mode for our sample types. The use of the 'Mining' mode also allowed us to adjust the calibration curve. This is particularly important because the matrix of meteorites differs from common terrestrial rocks.

The user has no access to the detailed algorithms used for quantification including inter-element corrections. For this reason, we are not able to treat these issues here in detail, but the instrument user can optimize the accuracy by adjusting the calibration curves as discussed in the Section on Calibration Correction Factors.

The instrument was originally designed for field use, but it can also be mounted in a portable test stand and be controlled by an external computer for nondestructive 'laboratory' analyses. The values of the measured elements appear in real time on the instrument's LCD display (touch screen) or on the screen of a connected computer. All concentrations are displayed as elements, not oxides, as commonly used in geology. Therefore, all data are listed here in elemental form.

Standard samples

In order to define optimal analytical conditions and to test the quality of the instrument, a set of standard samples was analyzed using alternating measuring times. In the first step, we used international (TILL-4, NCS DC 73308, NIST 2780 and RCRA) and in-house (KAI 230 R, MPI olivine sand, MPI norite, MPI diabase and Desert Soil 0603-062b) standards to test the accuracy of the method (Table 2). Meteorites are richer in iron and denser (higher average Z) in comparison to soils and most terrestrial rocks. Therefore, a modification of the calibration of the instrument is needed; this can easily be achieved by adjustment of the slope of the calibration curve for the 'Mining' mode of our instrument. For this purpose, a series of meteorites with well-known compositions were measured with 'factory settings' and compared with values obtained by other methods such as ICP-MS, ICP-OES or XRF mainly carried out by Activation Laboratories [Ancaster, Ontario, Canada (Actlab)], (Table 3), in order to test the applicability of the 'factory' settings for meteorite analysis. This allows the calculation of correction factors for each element of interest for a proper calibration. We used meteorite powders mounted in standard X-ray sample cups, meteorite powders prepared as pressed pellets and meteorite hand specimens for calibration and for testing the robustness of our procedure. By measuring hand specimens of meteorites, we tested the degree of natural variation within single samples. As meteorite standard samples, ordinary chondrites found in Oman (JaH 091, Shalim 004, AH 010 and UaH 001) were mainly used because these are the main objects for future studies. Additionally, three achondrites were tested: ureilite SaU 511, martian meteorite SaU 094[27] and lunar meteorite SaU 169[28] because their compositions are distinct from chondrites. Finally, we also included powders and hand specimens of Allende, a carbonaceous chondrite (type CV3) that fell on 8 February 1969.[29] This is one of the best studied meteorites with well-established concentration ranges, used in several laboratories as standard material.[30] Elements of main interest for our study are K, Ca, Ti, Cr, Mn, Fe and Ni as important primary elements in meteorites that can be used for identification and chemical classification of meteorites,[31,32] and Sr and Ba, as important contaminants from the soil in hot desert meteorites (e.g. see Stelzner *et al.*,[33] and Al-Kathiri *et al.*,[34]). For the test measurements, meteorites with the highest available variability in composition were used with the intention to cover the whole range of meteoritic compositions. For Sr and Ba, spiked chondrite pressed pellets were produced in addition to natural samples to enlarge the concentration range. Finely ground JaH 091, a L5 ordinary chondrite,[35,36] was used as matrix material. Pure Ba carbonates and Sr carbonates were used for spiking and sodium glass (water glass, which bears Na and K) as cement in the pressed pellets.

Shielding depth experiments

Most meteorites are medium-grained to fine-grained rocks with typical mineral grain diameters of 0.01 to 1 mm. Variations in composition can occur within a few millimeters, either as a result of primary inhomogeneities, especially the presence of up to mm-sized grains of Fe–Ni metal and Fe-sulfide, or as a result of

Table 2. List of international and in-house standards (STD)

Sample	Class	Source	K	Ca	Ti	Cr	Mn	Fe	Co	Ni	Sr	Sr[a]	Ba
TILL-4	Int STD	Niton Manual	27 000	8 900	4 840	53	490	39 700	8	17	109		395
NCS DC 73308	Int STD	Niton Manual	1 041	2 800	1 270	136	1 010	27 000	15.3	30	25		42
NIST 2780	Int STD	Niton Manual	33 800	1 950	6 990	44	462	27 840	2.2	12	217		993
RCRA	Int STD	Niton Manual				500							100
KAI 230 R, soil sample	In-house STD	Actlab, MPI	49 850	19 767	4 967	119	612	45 475	17	54	166		461
MPI olivine sand	In-house STD	MPI	166	2 644	119.9	2 090	820.97	54 133.56	194	2 620	12		20
MPI norite	In-house STD	MPI	2 491	89 123	893.255	30	999.105	42 943.16	125	100	316		101
MPI diabase	In-house STD	MPI	3 487	51 673	9 681.925	270	1 425.08	82 739.02	86	140	476		130
Desert Soil 0603-62b	In-house STD	Actlab	8 551	146 299	5 647.29	2 870	596.365	20 002.84	16	110	382	363	240

All values in p.p.m.
[a]X-ray fluorescence.

Table 3. List of the meteorites and element concentrations used as standards for instrument calibration

Sample	Class	Source	K	Ca	Ti	Cr
AH_010 (0201_791)	L	Al-Kathiri 2005	996 ± 100	12 579 ± 800	611 ± 100	3 050 ± 200
AH_011 (0201_0788)	L	Al-Kathiri 2005	779 ± 100	12 506 ± 800	678 ± 100	4 000 ± 200
Allende (2010)	CV	Actlab	415 ± 100	17 081 ± 800	803 ± 100	3 390 ± 200
Allende (2009)	CV	Actlab	830 ± 100	16 438 ± 800	791 ± 100	3 360 ± 200
Allende Jarosewich	CV	Jarosewich 1987	332 ± 100	18 439 ± 700	899 ± 100	3 626 ± 200
Dho_813 (0101_163)	L	Al-Kathiri 2005	1 085 ± 100	16 249 ± 800	705 ± 100	4 180 ± 200
JaH_069 (0101_008)	H	Al-Kathiri 2005	963 ± 100	14 789 ± 800	684 ± 100	4 410 ± 200
JaH_091 Med	L	Calc [b]	1 328 ± 100	12 865 ± 800	647 ± 100	3 310 ± 200
JaH_091 (0201_011) [2009]	L	Actlab	996 ± 100	12 007 ± 800	594 ± 100	3 430 ± 200
JaH_091 (0210_0011B)	L	Al-Kathiri 2005	789 ± 100	11 037 ± 800	519 ± 100	3 360 ± 200
JaH_091 (0210_011) [2010]	L	Actlab	830 ± 100	12 436 ± 800	629 ± 100	3 400 ± 200
JaH_091 AM	Spiked L	Calc				
JaH_091 M1	Spiked L	Calc				
JaH_091 M2	Spiked L	Calc				
JaH_091 M3	Spiked L	Calc				
JaH_091 STD	Spiked L	Calc				
JaH_091 ZMV	Spiked L	Calc				
SaU_194 (0102_227)	L	Al-Kathiri 2005	991 ± 100	13 672 ± 800	665 ± 100	3 630 ± 200
SaU_511 (0902_018)	Ureilite	Al-Kathiri 2005	83 ± 100	13 508 ± 800	264 ± 100	4 260 ± 200
Shalim _003	H	Al-Kathiri 2005	619 ± 100	12 259 ± 800	659 ± 100	3 500 ± 200
Shalim_004 (0103_259)	H	Al-Kathiri 2005	1 411 ± 100	11 864 ± 800	540 ± 100	2 540 ± 200
Shalim_004 am	Spiked H	Calc				
Shalim_004 m1	Spiked H	Calc				
Shalim_004 m2	Spiked H	Calc				
Shisr_020 (0102_256)	H	Actlab	818 ± 100	14 749 ± 800	653 ± 100	4 160 ± 200
UaH_001 (0301_0003)	LL	Actlab	1 245 ± 100	13 222 ± 800	695 ± 100	3 500 ± 200
SaU_169 IMB	Lunar	Gnos 2004	4 480 ± 100	72 614 ± 800	13 249 ± 200	975 ± 200
SaU_169 Rego	Lunar	Gnos 2004	7 310 ± 100	75 758 ± 800	8 813 ± 200	816 ± 200
SaU_094	Martian	Actlab	747 ± 100	43 954 ± 800	2 332 ± 200	5 650 ± 200

All values in p.p.m.
[a]X-ray fluorescence.
[b]Calc = calculated.

the presence of contamination-rich surface rinds when measuring meteorite surfaces. It is important to know the effective depth of analysis and its consequences for analytical results. To explore this issue, a test series has been designed. Natural minerals extremely rich in certain key elements (i.e. not pure chemical end members) were selected, and the X-ray intensities of these elements were measured through a pile of 1 up to 15 slices of ordinary chondrite [unclassified chondrite from Northwest Africa (NWA), H-type] with thicknesses ranging from 0.4 to 0.75 mm, summing up to a total chondrite thickness of 8.32 mm (Tables 4 and 5). Counting times of 300 s were used, in the case of Ba, to put down the detection limit (DL) of Ba to ~100 p.p.m.; all other elements were measured for 180 s because the high filter is not used.

Results

Influence of the sample type

Most standards used are samples with at least one flat surface: powders mounted in standard XRF cups or as pressed pellets and hand specimens with cut surfaces (CSs). Nevertheless, some irregularly shaped samples were also measured, especially hand specimens from Allende and the convex side of pressed pellets. No significant or specific differences were observed between powdered samples (pressed into pellets and loose in sample cups) and hand specimens, both using flat and rough surfaces on the latter. In hand specimens, variations can occur on irregular or rough surfaces but are interpreted as natural inhomogeneities. Repeated measurements on uniform samples with the 8-mm window mode and subsequent 3-mm small spot mode yielded similar concentrations within two sigma error. The variation of accuracies of the different sample types is listed in Table 6.

Signal depth of contaminants

The experiments measuring the maximum depth, from which a characteristic X-ray signal of a contaminant can be obtained while shielded with meteorite material, yielded some interesting results. Because meteorites have a very dense matrix, small critical depths are expected. Indeed, calculations of penetration depth (minimum thickness of sample to obtain correct values) using H-chondrite composition[37] and a density of 3.4 g/cm^3 [38] yield values below or around 1 mm for chromium ($K\alpha_1$ at 5.4 keV), manganese ($K\alpha_1$ at 5.9 keV), iron ($K\alpha_1$ at 6.4 keV) and Sr ($K\alpha_1$ at 14.2 keV). Barium ($K\alpha_1$ at 32.2 keV) has a calculated penetration depth of about 3 mm. This is also visible in the shielding experiment (Fig. 1), but the contribution of the contaminants behind the meteorite slices seems to be derived from a greater

Table 3. (*Continued*)

Cr [a]	Mn	Fe	Co	Ni	Sr	Sr [a]	Ba
3 590	2 517 ± 100	200 380 ± 1 000	560 ± 100	11 500 ± 200	14 ± 3	11 ± 3	9 ± 3
	2 151 ± 100	230 000 ± 1 000	571 ± 100	10 800 ± 200	25 ± 3		7 ± 3
	1 456 ± 100	234 580 ± 1 000	435 ± 100	2 790 ± 200	14 ± 3		7 ± 3
	1 441 ± 100	236 820 ± 1 000	570 ± 100	9 390 ± 200	15 ± 3		6 ± 3
	1 472 ± 100	235 700 ± 800	600 ± 100	14 200 ± 200	12 ± 3		4 ± 1
	2 295 ± 100	238 000 ± 1 000	601 ± 100	10 000 ± 200	1 140 ± 3		150 ± 20
	1 974 ± 100	303 000 ± 1 000	750 ± 100	13 200 ± 200	594 ± 3		150 ± 20
	2 494 ± 100	207 440 ± 1 000	567 ± 100	± 200	15 ± 3		7 ± 3
3 890	2 432 ± 100	214 580 ± 1 000	580 ± 100	11 900 ± 200	13 ± 3	14 ± 3	4 ± 3
	1 982 ± 100	204 000 ± 1 000	550 ± 100	11 900 ± 200	14 ± 3		3 ± 3
	2 517 ± 100	204 710 ± 1 000	432 ± 100	5 100 ± 200	12 ± 3		8 ± 3
					21 818		3 285 ± 300
					670		105 ± 10
					233		39 ± 15
					123		22 ± 8
					14		6 ± 3
					2 008		306 ± 15
	2 001 ± 100	240 000 ± 1 000	644 ± 100	13 600 ± 200	181 ± 3		73 ± 15
	3 059 ± 100	145 970 ± 1 000	125 ± 30	1 380 ± 200	86 ± 3		32 ± 7
	2 066 ± 100	241 000 ± 1 000	780 ± 100	14 500 ± 200	19 ± 3		5 ± 3
3 770	2 308 ± 100	229 260 ± 1 000	700 ± 100	14 800 ± 200	13 ± 3	11 ± 3	5 ± 3
					100 010		10 015
					3 014		357
					1 014		156
	1 874 ± 100	296 000 ± 1 000	733 ± 100	13 200 ± 200	938 ± 3		265 ± 20
	2 688 ± 100	175 830 ± 1 000	459 ± 100	8 660 ± 200	22 ± 3		5 ± 3
	1 084 ± 100	82 938 ± 1 000	31 ± 10	204 ± 50	359 ± 20		1 520 ± 40
	929 ± 100	68 402 ± 1 000	19 ± 8	58 ± 15	214 ± 15		593 ± 30
	3 570 ± 100	140 070 ± 1 000	63 ± 12	311 ± 50	83 ± 3		68 ± 15

Table 4. Thicknesses of slices used for the shielding experiments

MJA label	Thickness of slice [mm]	Shielding thickness[a] (mm)
A	0.40	0.40
B	0.43	0.83
C	0.50	1.33
D	0.50	1.83
E	0.54	2.37
F	0.55	2.92
G	0.55	3.47
H	0.55	4.02
I	0.55	4.57
J	0.57	5.14
K	0.60	5.74
L	0.60	6.34
M	0.60	6.94
N	0.63	7.57
O	0.75	8.32

[a]During the experiments the slices were placed in alphabetical order. Shielding thickness is the resulting cumulative thickness of meteorite slices between the handheld X-ray fluorescence and the test mineral.

Table 5. Minerals and instrument conditions used for determination of depth of interaction for different elements (contaminants)

Element	Tube conditions	Mineral	Idealized chemical formula	Signal depth (mm)
Cr	20 kVp, 100 μA	Chromite	$FeCr_2O_4$	<1
Mn	40 kVp, 50 μA	Mn-ore	MnO2	<1
Fe	40 kVp, 50 μA	Magnetite	Fe3O4	<1
Sr	40 kVp, 50 μA	Celestine	SrSO4	<2
Ba	50 kVp, 40 μA	Barite	BaSO4	<5

depth, especially in the case of Ba, where it is still overestimated behind ~5 mm of meteorite material. Strontium is also measured from greater depths. These two elements have higher penetration depths because they have also higher activation energies. They might be detected deeper because they are only present as traces in the chondrite but highly concentrated in the material behind the meteorite slices. While the calculated penetration depth determines the minimum thickness of a sample to obtain correct values, our experiment delivers the maximum depth from which a specific element signal can be derived through a

Table 6. The elements of interest

Element	Correction factor 'factory'	Correction factor 'meteorite'	Correction factor 'desert soil'	Precision[a] HHXRF (%)	Accuracy[b] HHXRF (%)	Accuracy HHXRF HS[c] (%)	Accuracy HHXRF PH[d] (%)	Accuracy HHXRF pp[e] (%)	Detection limits[f] (p.p.m.)
K	1	0.98	1.08	8.4	18.0	11.4	18.0	—	500
Ca	1	1.13	0.87	2.8	15.1	16.6	12.1	—	—
Ti	1	1.40	1.55	0.3	10.8	14.2	6.4	—	200
Cr	1	1.13	1.50	0.9	17.8	22.0	12.0	(19.5)	80
Mn	1	0.98	0.99	0.8	16.1	16.1	8.3	(16.2)	70
Fe	1	1.04	1.10	0.8	7.0	8.8	7.0	(1.4)	300
Co	1	1.20	—	—	30.5	12.4	29.5	(40)	400
Ni	1	1.36	1.03	2.5	9.1	17.3	5.0	—	20
Sr	1	1.60	1.70	2.7	11.2	20.3	6.0	19.4	6
Ba	1	1.04	2.20	—	16.3	26.5	71.2	5.3	100
Average all	1	1.19	1.34	2.4	15.2	16.6	17.5		

Correction factors used for meteorite and desert soil samples, precision, accuracies and detection limit for the element of interest at 300-s measurements.

[a]Precision: three to five repeated measurements at the very same spot from two different samples; deviation in % to the median value of measurements.

[b]Accuracy: deviation of handheld X-ray fluorescence (HHXRF) (y) from standard/reference value (x) [literature, ICP-MS, X-ray fluorescence (XRF)], $((x-y)/x)*100$), medians from 5 to 51 measurements, including all kind of samples.

[c]HS: hand specimen, measurements mainly at cut surface (CS).

[d]PH: measurements of powder in XRF standard cups.

[e]pp: spiked powder press pellets, standard values for Ba and Sr are calculated.

[f]Detection limits observed measuring standard samples, meteorites, soil samples or marbles.

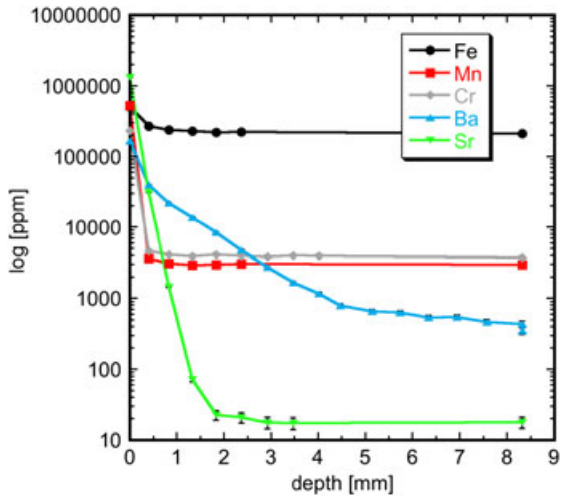

Figure 1. Maximum depth of contaminant signal provenance for Fe $K\alpha_1$, Mn $K\alpha_1$, Cr $K\alpha_1$, Ba $K\alpha_1$ and Sr $K\alpha_1$. Minerals with high concentrations of the respective element were covered with thin meteorite slices of variable thickness. Excess Fe, Mn and Cr were detected through a meteorite cover of 1 mm, whereas excess Ba was still detected when 5 mm of meteorite shielding was present between the detector and the barite. A constant value is reached because of the contribution of the meteorite slices.

chondrite. The implication of our experiment is that signals of most of the contaminants tested in the experiment are derived from low depths (<1 mm) with the exception of Sr and Ba, which contribute up to depths of 2 mm and 5 mm, respectively (Table 5).

Precision and required counting times

Precision is dependent on signal intensity and counting time and varies from element to element. The tested HHXRF instrument lists an element as detected when the standard deviation error of the result has decreased to <30% of the measured value. Most of the typical meteoritic elements (Ca, Ti, Mn, Fe, Ni and Sr) are detected at the expected range using counting times of about 10 to 25 s. Other elements such as K, Co and Ba require longer measuring times. Because for field applications (as discussed in the Section on Identification of Doubtful Meteorites), only Ca, Mn, Fe, Ni and Sr are of key interest, the measuring time can be accordingly reduced for such applications. We recommend a 'field setup' of at least 60-s total measuring time where 30 s are measured with the 'main filter' and 30 s with the 'low filter', respectively. With this setup, the errors of the most important elements for field issues are in an acceptable range (<20% deviation). Because Ba is not needed for field applications, the 'high filter' is switched off. In contrast, with the use of a 'lab setup' where also data for K, Ti, Co and especially Ba are desired, a counting time of 300 s using the 'Mining' mode is recommended. A counting time of 120 s using the 'main filter' is important because the background correction and the virtual element are calculated on the basis of data collected with this filter. For 'low filter', 60 s is sufficient while 120 s for 'high filter' is needed to decrease the DL of barium particularly. For a fatigue-proof handheld measurement (Fig. 2) on a small sample, 300 s is too long. For this reason, the device is mounted on a test stand with a shielded box protecting the user from stray radiation. Samples are set on a horizontal table and, in the ideal case, have a flat surface and do not exceed the dimensions of the 19 cm 19 cm × 10 cm shielded box.

Calibration correction factors

Several meteorite samples, including powders, pressed pellets and hand specimens, were measured for 300 s, and with the deviation of the HHXRF data from the 'standard' value, correction

factors were calculated (Table 6). Some results were excluded from the calculations, as they did not fit to the standard value for explicable reasons. For example, K contents measured on the pressed pellets were too high because of K from sodium silicate (water glass) used for cementation. At high Ba concentrations (~400 p.p.m. Ba), the Ti $K\alpha$ and Ba $L\alpha$ peak overlap has an influence, resulting in overestimated Ti concentrations (Fig. 3). This overlap cannot be corrected by adjustment of a calibration curve. Repeated measurements of the same powder of Allende by ICP-MS, ICP-OES and XRF yielded some slight but relevant differences for some elements [i.e. K and Ni concentrations of Allende (2009) and Allende (2010), Table 3]. When calculating the correction factors, such strong outliers were excluded. The production of meteorite powder is a difficult issue because most of the meteorites contain metallic iron that is tricky to grind resulting in non-uniform powders sometimes containing metal 'nuggets'. Nickel and cobalt are concentrated in the iron metal grains and hence typically yield low values. When hand specimens are measured, it has to be taken into account that minerals such as chromite (Cr-rich) or Ca-rich minerals such as feldspars or Ca-rich pyroxenes are not distributed homogeneously in a sample. This is also the case for terrestrial contamination minerals such as calcite, gypsum (both Ca-rich) or barite ($BaSO_4$) and celestite ($SrSO_4$). Even with the spot size of 8 mm, those effects can locally influence the measurement. The inhomogeneous distribution of Sr on a large cut slab of Allende is displayed in Fig. 4. Because this is an observed meteorite fall unaffected by weathering, the variation of Sr is a primary effect and not due to contamination. Strontium is related to Ca-bearing minerals, such as Ca-rich pyroxene, feldspar (or feldspatic glass) Ca-phosphate and Ca–Al-rich inclusions, which are not distributed homogeneous in the relatively coarse-grained Allende meteorite.

Figure 2. *In situ* handheld X-ray fluorescence analysis of a meteorite (RaS 309) discovered in the desert of Oman. Note the high contrast between the dark meteorite and the light colored soil.

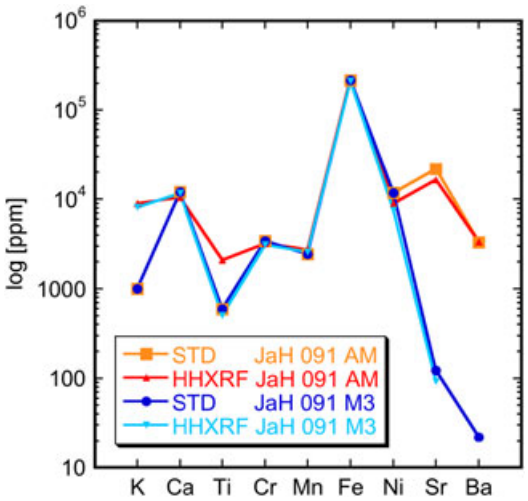

Figure 3. Data for two samples (median values of 4 HHXRF measurements) of Ba-spiked and Sr-spiked standard pressed pellets compared with expected values (STD). In the high Ba sample JaH 091 AM, the Ti content is overestimated because of overlapping of Ti $K\alpha$ and Ba $L\alpha$ lines. Note the elevated K values observed in the pressed pellets produced with sodium silicate (water glass).

The results of the corrected measurements are presented in Table 7. Most meteorites have comparable 'chondritic' bulk compositions. Their mineralogy is dominated by olivine $(Mg, Fe)_2SiO_4$, Ca-poor pyroxene $(Mg, Fe)SiO_3$ and Ca-rich pyroxene $(Ca, Mg, Fe)SiO_3$, feldspar $(Ca, Na, K)(Si, Al)_4O_8$, Ca-phosphate $Ca_5(PO_4)_3(F, OH, Cl)$, iron sulfide (FeS) and metallic iron–nickel, kamacite and taenite (Fe, Ni) and Cr-rich spinel $(Fe, Mg)(Cr, Al)_2O_4$, (e.g. see McSween *et al.*,[39] and Rubin[40]). Therefore, the correction factors are valid for most of the stony meteorite types.

In addition to meteorite samples, a series of soil samples from Oman were measured, and correction factors were calculated for this type of samples (Table 6). Because the instrument is calibrated with an FP for common geological samples, small calibration adjustments are required for desert soil samples to fit with standard values.

Discussion

Accuracy, precision and detection limits

The instruments precision is of high quality for a field portable device. Precision was determined by three to five repeated

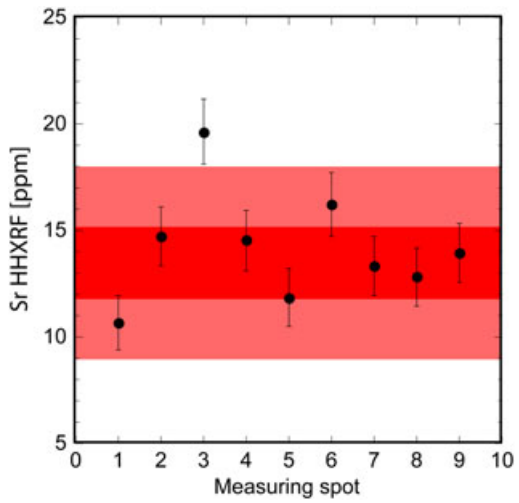

Figure 4. Strontium variation in a large cut slab of the Allende CV3 meteorite. All data points represent measurements of 300 s. Dark red: all available reference values[30] (Actlab 2009 & 2010); light red: corresponding error box. Sr is not homogeneously distributed in meteorites. Therefore, we recommend using weighted mean values.

Table 7. Handheld X-ray fluorescence (HHXRF) measurements of meteorite samples

Sample	Sample status[a]	Sample surface[b]	Measuring mode[c]	Number of analyses	K	Ca	Ti
AH_010	PH	P	ModCF Meteorit-8 mm	2	n.d. < 796	14 044 ± 474	628 ± 75
AH_010 std	pp	gp	ModCF Meteorit-8 mm	3	n.d. < 1 390	11 786 ± 491	555 ± 70
AH_011 (0201_788)	HS	CS	ModCF Meteorit-8 mm	5	494 ± 621	13 863 ± 471	578 ± 75
Allende	HS	NS	ModCF Meteorit-8 mm	5	n.d. < 832	21 219 ± 594	906 ± 87
Allende M13	PH	P	ModCF Meteorit-8 mm	3	n.d. < 793	18 429 ± 563	752 ± 85
Dho_813 (0101_163)	cs	cs	ModCF Meteorit-8 mm	3	672 ± 607	21 219 ± 632	672 ± 76
JaH_069	HS	NS	ModCF Meteorit-8 mm	5	n.d. < 451	11 240 ± 428	855 ± 81
JaH_069 (0101_008D)	HS	CS	ModCF Meteorit-8 mm	6	1 073 ± 403	14 819 ± 454	691 ± 73
JaH_091	PH	P	ModCF Meteorit-8 mm	3	n.d. < 849	14 593 ± 486	656 ± 77
JaH_091 AM	pp	gp	ModCF Meteorit-8 mm	4	4 784 ± 595	11 448 ± 446	2 742 ± 124
JaH_091 M1	pp	gp	ModCF Meteorit-8 mm	4	3 402 ± 551	14 421 ± 491	701 ± 79
JaH_091 M2	pp	gp	ModCF Meteorit-8 mm	4	20 379 ± 1 017	12 561 ± 479	655 ± 76
JaH_091 M3	pp	gp	ModCF Meteorit-8 mm	4	30 239 ± 1 206	12 948 ± 502	652 ± 76
JaH_091 STD	pp	gp	ModCF Meteorit-8 mm	4	7 954 ± 693	13 435 ± 467	568 ± 72
JaH_091 ZMV	pp	gp	ModCF Meteorit-8 mm	4	6 704 ± 656	13 610 ± 471	797 ± 79
SaU_194	PS	P	ModCF Meteorit-8 mm	3	n.d. < 758	13 362 ± 445	591 ± 70
SaU_194	HS	CS	ModCF Meteorit-8 mm	3	n.d. < 785	17 236 ± 512	842 ± 79
SaU_194	HS	NS	ModCF Meteorit-8 mm	5	n.d. < 459	19 708 ± 552	n.d. < 85
SaU_194 (0102_227)	HS	CS	ModCF Meteorit-8 mm	3	995 ± 416	18 037 ± 537	723 ± 75
SaU_511 (0901_018)	HS	CS	ModCF Meteorit-8 mm	3	n.d. < 260	12 743 ± 171	267 ± 22
Shalim_004 (0203_259)	HS	CS	ModCF Meteorit-8 mm	3	n.d. < 638	15 476 ± 444	766 ± 64
Shalim_004 am	pp	gp	ModCF Meteorit-8 mm	4	11 683 ± 982	10 739 ± 545	7 697 ± 274
Shalim_004 m1	pp	gp	ModCF Meteorit-8 mm	4	97 672 ± 2 035	7 609 ± 519	452 ± 68
Shalim_004 m2	pp	gp	ModCF Meteorit-8 mm	4	130 900 ± 2 326	2 419 ± 504	340 ± 65
Shalim_004 oman	PH	P	ModCF Meteorit-8 mm	3	n.d. < 764	13 517 ± 472	663 ± 78
Shalim_004 std	pp	gp	ModCF Meteorit-8 mm	4	66 654 ± 1 695	6 908 ± 460	n.d. < 66
Shisr_020	PH	P	ModCF Meteorit-8 mm	4	n.d. < 859	17 878 ± 556	804 ± 87
Shisr_020 (0102_256)	cs	CS	ModCF Meteorit-8 mm	3	n.d. < 824	12 365 ± 467	714 ± 79
UaH_001 (0301_0003)	PH	P	ModCF Meteorit-8 mm	3	1 469 ± 435	17 398 ± 507	771 ± 74
UaH_001 (0301_0003)	HS	CS	ModCF Meteorit-8 mm	4	1 162 ± 406	17 677 ± 509	792 ± 73
SaU_169 IMB	HS	CS/NS	ModCF Meteorit-8 mm	4	5 059 ± 320	74 117 ± 1 050	16 175 ± 363
SaU_169 Regolith	HS	CS/NS	ModCF Meteorit-8 mm	6	6 783 ± 532	88 320 ± 1 122	n.d. < 367
SaU_094	HS	CS	ModCF Meteorit-8 mm	5	2 033 ± 1 323	45 091 ± 810	2 585 ± 104

[a]PH: powder in standard XRF cup, pp: pressed pellet, HS: hand specimen, cs: small hand specimen.
[b]P, powder; gp, water glass cemented powder; CS, cut surface; NS, natural surface; n.d., not detected.
[c]All measurements with modified calibration factor (ModCF) for meteorites ('Meteorite') with a spot size of 8 mm.
All values in p.p.m.

measurements at the very same spot of two different international standards at counting times of 300 s each. Potassium has the lowest precision of 8.4%; all other studied elements range between 0.8% and 2.8%. The calculation of the accuracy is not an easy task. For example, an offset of the standard value obtained by Activation Laboratories, in comparison to the values recommended by Jarosewich and coauthors,[30] was observed for the Allende standard samples. The powder used for the Actlab analysis was from a small fragment (approx 1.5 g) that might be biased because the components of Allende are relatively coarse. The mean chondrule diameter is around 1 mm (variance 0.5–2 mm),[29] responding to the observed dependence of grain size of the contaminants in soils and the needed sample mass to get representative results; the mass should have been >6 g (see Eggimann[41] and the references therein). Because we are interested mainly in the major and some trace elements that are distributed nearly homogeneous (with the exception of Cr) in the sample, we believed to have an adequate sample mass. The used Oman meteorite standard samples were available in larger quantities and repeated measurements by Actlab yielded similar concentrations. The accuracy was calculated using the deviation of the adjusted HHXRF measurements from the standard values. Each standard sample was measured with HHXRF for at least three times, and the median out of these measurements was taken for the calculation. The relative errors for the elements of interest are 10% to 20%, which is considered acceptable for a field portable instrument (Table 6).[2]

The best results were obtained for iron, which is the element occurring at the highest concentrations. The rather large errors for Co and Ni could be due to the inhomogeneous distribution of iron particles and the high absorption of X-rays within the metallic iron particles. By measuring pressed pellets with high concentrations of Sr, a large offset was observed. This is due to the large uncertainty on the standard value and the apparent nonlinear behavior of Sr at concentrations exceeding 1000 p.p.m. Only linear corrections are possible with the used HHXRF analyzer.

Table 7. (*Continued*)

Cr	Mn	Fe	Co	Ni	Sr	Ba
3 697 ± 110	2 614 ± 135	217 800 ± 3 050	n.d. < 360	11 549 ± 226	11 ± 1	n.d. < 83
3 160 ± 100	2 324 ± 127	187 260 ± 2 618	743 ± 171	23 152 ± 388	12 ± 1	n.d. < 82
2 924 ± 101	2 725 ± 135	210 470 ± 2 922	n.d. < 337	9 290 ± 187	12 ± 1	n.d. < 84
4 491 ± 126	1 498 ± 117	245 520 ± 3 495	n.d. < 380	12 308 ± 247	17 ± 1	n.d. < 91
4 378 ± 127	1 560 ± 121	252 160 ± 3 668	583 ± 198	13 270 ± 270	13 ± 1	n.d. < 89
4 378 ± 92	2 345 ± 130	258 480 ± 3 737	578 ± 195	10 610 ± 223	888 ± 15	118 ± 47
2 388 ± 94	2 889 ± 141	267 180 ± 3 829	n.d. < 400	15 926 ± 318	548 ± 10	99 ± 47
2 940 ± 99	2 291 ± 135	268 830 ± 3 899	n.d. < 407	12 796 ± 273	333 ± 8	n.d. < 98
4 083 ± 117	2 523 ± 135	221 230 ± 3 124	388 ± 182	10 087 ± 205	15 ± 1	n.d. < 86
3 809 ± 119	2 714 ± 179	228 080 ± 3 985	483 ± 238	12 186 ± 300	27 849 ± 487	3 400 ± 136
3 866 ± 114	2 722 ± 139	223 760 ± 3 161	n.d. < 367	10 800 ± 217	733 ± 12	107 ± 45
3 540 ± 109	2 494 ± 133	215 840 ± 3 059	483 ± 181	10 901 ± 215	249 ± 5	n.d. < 85
3 512 ± 109	2 512 ± 134	216 350 ± 3 086	553 ± 182	10 192 ± 203	200 ± 5	n.d. < 84
3 670 ± 108	2 418 ± 130	212 960 ± 2 943	n.d. < 350	9 681 ± 192	15 ± 1	n.d. < 84
3 597 ± 108	2 498 ± 134	210 400 ± 2 950	405 ± 179	9 796 ± 197	2 475 ± 35	328 ± 46
3 607 ± 105	2 418 ± 130	254 240 ± 3 503	n.d. < 377	13 490 ± 262	178 ± 4	125 ± 51
3 377 ± 103	2 374 ± 129	213 760 ± 2 931	n.d. < 348	5 828 ± 132	92 ± 3	n.d. < 85
2 786 ± 95	3 155 ± 146	233 110 ± 3 319	n.d. < 375	7 564 ± 168	546 ± 10	n.d. < 46
3 026 ± 96	2 449 ± 131	223 650 ± 3 136	n.d. < 355	5 138 ± 124	87 ± 3	n.d. < 87
5 105 ± 49	2 901 ± 54	169 900 ± 900	n.d. < 120	1 715 ± 25	76 ± 1	125 ± 17
2 983 ± 99	2 536 ± 136	235 980 ± 3 358	n.d. < 380	10 667 ± 221	14 ± 1	n.d. < 100
3 753 ± 165	2 747 ± 320	252 620 ± 7 190	1 203 ± 437	20 210 ± 747	164 020 ± 5 063	13 634 ± 860
2 571 ± 94	1 977 ± 128	194 820 ± 2 931	1 561 ± 193	53 144 ± 896	3 467 ± 52	359 ± 49
2 295 ± 90	1 968 ± 127	198 040 ± 2 982	1 564 ± 192	47 401 ± 794	1 461 ± 23	135 ± 45
3 793 ± 114	2 437 ± 133	242 610 ± 3 431	520 ± 191	14 635 ± 284	12 ± 1	n.d. < 90
3 033 ± 102	1 935 ± 124	226 090 ± 3 270	980 ± 190	27 745 ± 484	17 ± 1	n.d. < 88
4 061 ± 123	2 278 ± 136	273 860 ± 4 039	637 ± 208	13 871 ± 290	995 ± 17	n.d. < 92
3 492 ± 114	2 400 ± 138	246 060 ± 3 621	824 ± 199	12 373 ± 259	16 ± 1	n.d. < 92
4 116 ± 111	3 158 ± 144	189 140 ± 2 613	n.d. < 334	4 178 ± 104	24 ± 1	n.d. < 81
2 629 ± 90	3 123 ± 140	175 190 ± 2 377	n.d. < 315	3 513 ± 89	26 ± 1	n.d. < 78
1 201 ± 64	1 280 ± 37	90 563 ± 877	n.d. < 325	216 ± 31	356 ± 6	1 230 ± 49
1 207 ± 97	1 207 ± 97	87 407 ± 1 270	n.d. < 348	78 ± 41	261 ± 5	515 ± 37
5 346 ± 125	3 688 ± 153	115 130 ± 2 033	n.d. < 305	281 ± 35	85 ± 3	n.d. < 88

For Sr concentrations, >1000 p.p.m. a second correction line is necessary. Accuracies for K, Co and Ba are to be taken with caution because these elements occur in meteorites in concentrations close to the DL of the used HHXRF. The other elements of interest (Ca, Ti, Cr, Mn, Fe, Ni and Sr) usually occur far above DL. Test on soil samples and other nonmeteoritic standards yielded element-specific DLs as noted in Table 6.

Evaluated elements

In the following section, elements of interest for meteorites and the corresponding soils are discussed following their Z number (Fig. 5):

Potassium

In most stone meteorites, potassium is a trace element (~50–8000 p.p.m.), often occurring close to the LOD of the HHXRF of around 500 p.p.m. (Fig. 5(a)). Potassium is concentrated in feldspar. For precise results, a minimum counting time of 60 s for the 'low filter' is recommended. The accuracy for K is about 18%, which is one of the worst. However, K is the lightest detectable element with the PIN detector under ambient conditions. Therefore, it is difficult to interpret K contents with respect to terrestrial contamination. For meteorite classification, only the order of magnitude is relevant.

Calcium

Calcium typically occurs in meteorites at concentrations of 1–2 wt %. We find a good agreement of our measurements with the independently determined values (Fig. 5(b)). Calcium is concentrated in plagioclase, Ca-rich pyroxenes and Ca-phosphate that are inhomogeneously distributed within meteorites. Therefore, some variation within a single sample is common. Additionally, Ca can occur as a terrestrial contaminant in the form of calcite or gypsum/anhydrite, mostly as vein.

Titanium

In chondritic meteorites, titanium is typically present at concentrations of 400 to 1200 p.p.m., most commonly 700–1100 p.p.m. Ti (Fig. 5(c)). The outliners on Fig. 5(c) are the measurements of the elative Ti-rich lunar meteorite SaU 169. Because of the methodology, a well-known overlap exists for the Ti $K\alpha$ and Ba $L\alpha$ lines. For common meteoritic concentrations, this is not a problem for the instrument used. Not until Ba exceeds concentrations of ~400 p.p.m., this overlap results in overestimated Ti values (Fig. 3).

Chromium

Meteorites generally have Cr concentrations of 1000–6000 p.p.m. with a peak of abundance at 3000–4000 p.p.m. (Fig. 5(d)). The main carrier phase is chromite, typically showing an irregular distribution in meteorites. Grain size is typically between 10 and 200 μm. In comparison with standard values, Cr measured by common XRF is mostly higher than the analysis by ICP-MS (Table 3). This could be due to insufficient leaching of chromite while sample preparation for ICP-MS.

We often observe an overestimation of Cr with HHXRF measurements that supports this conclusion. Because chromite is not distributed uniformly in unprepared natural samples, the Cr content often scatters by varying the measurement spot. The effective measuring depth for Cr is <1 mm. Therefore, it is important to measure at least three spots in hand specimens if proper Cr contents are required.

Manganese

Manganese is associated with Fe in silicate minerals, whereas the metal fraction of meteorites is devoid of Mn. In combination with Fe, Mn is an important element for the classification of

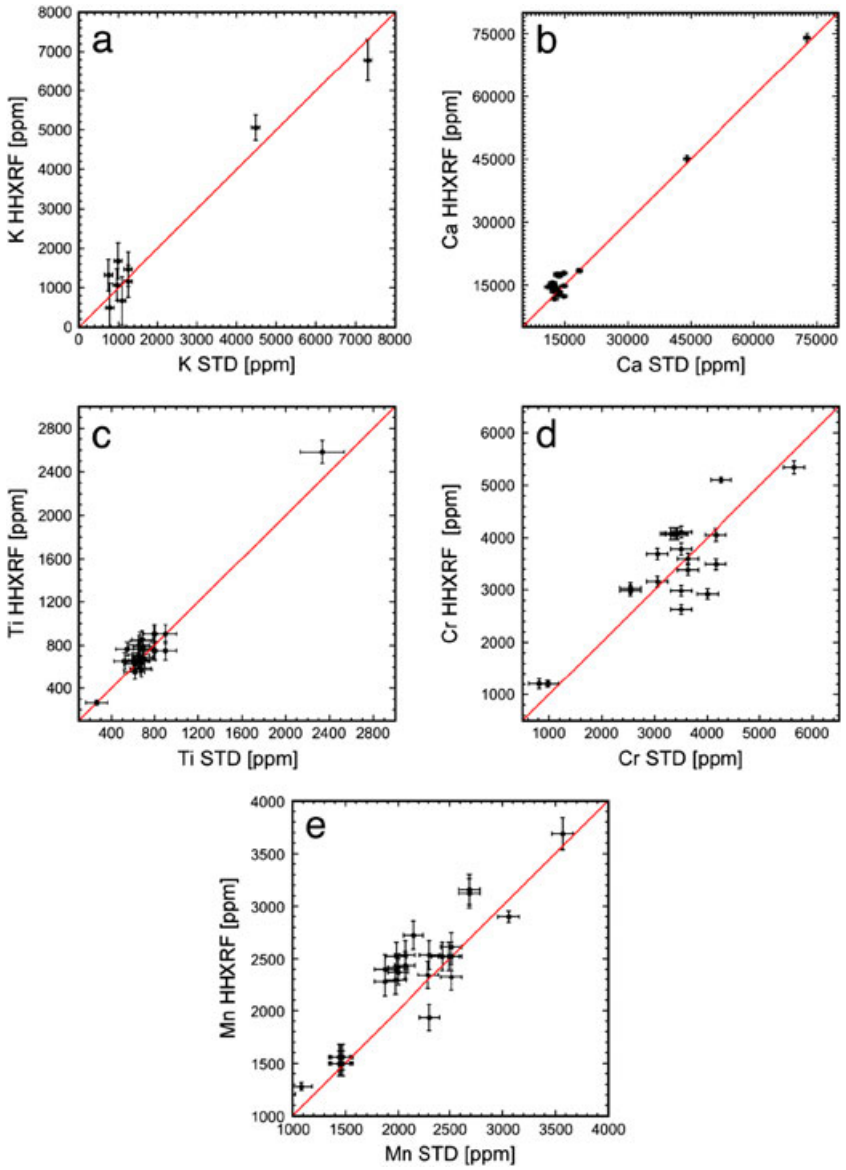

Figure 5. Handheld X-ray fluorescence (HHXRF) measurements on meteorite samples plotted *versus* reference (STD) values obtained by ICP-MS and XRF. (a) K, (b) Ca, (c) Ti, (d) Cr, (e) Mn, (f) Fe, (g) Co, (h) Ni, (i) Sr and (j) Ba. The red line shows 1:1 linear correlation. Note the logarithmic scale in the Ba, Ni and Sr plots.

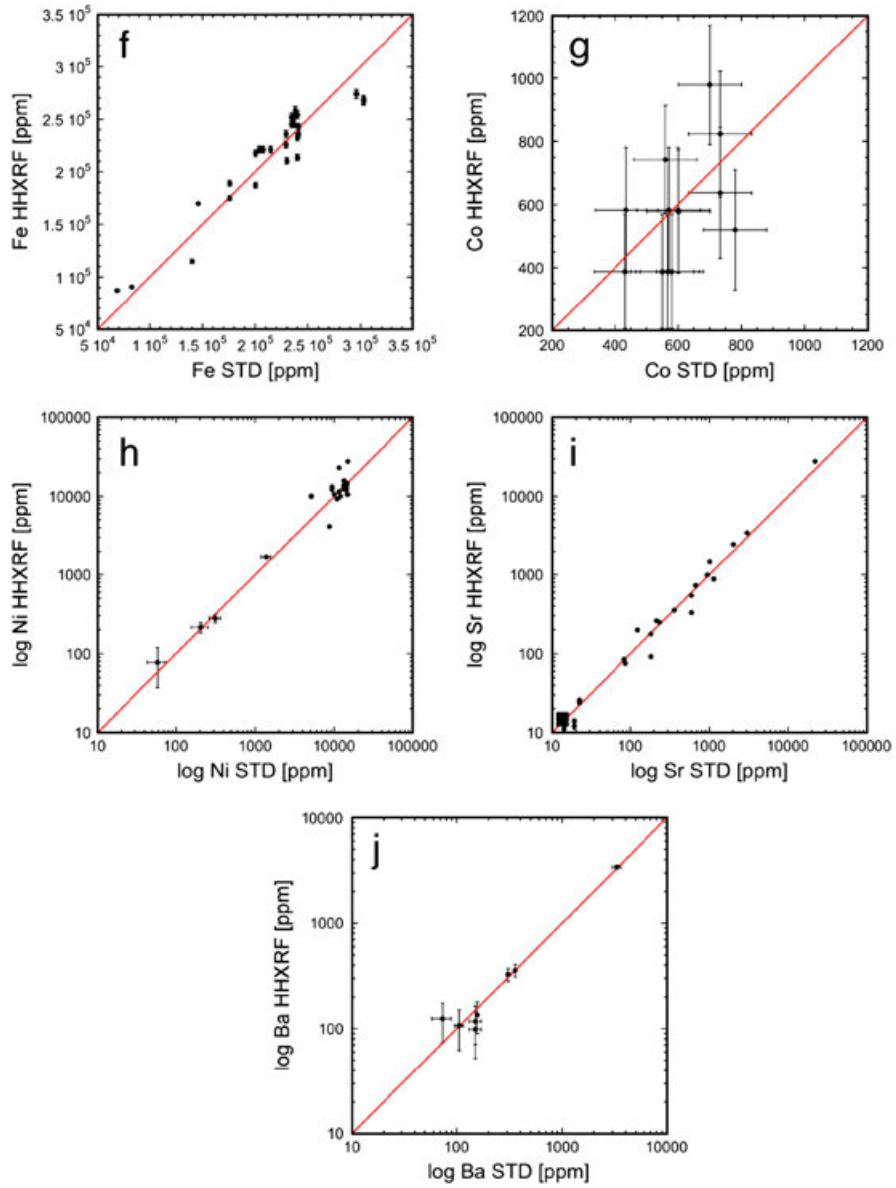

Figure 5. *(Continued)*

meteorites. Typical concentrations in silicate-rich meteorites are between 1000 and 4000 p.p.m. with a peak of values between 2200 and 2700 p.p.m. (ordinary chondrites and primitive achondrites) (Fig. 5(e)). No indications of a possible influence on analytical results of line interferences between Cr *Kß* and Mn *Kα* were observed during our survey. Similar to Cr and Fe, the effective measuring depth of Mn is <1 mm.

Iron

Iron is one of the most abundant elements in meteorites, ranging from <1 wt% in aubrites to ~90 wt% in iron meteorites. The most iron-rich ordinary chondrites contain up to 30 wt%. Up to this value, the instrument yields very good results (Fig. 5(f)). However, iron occurs partially in metallic form as 'nuggets' up to several millimeters that can cause X-ray absorption when measuring CSs of hand specimens and can be distributed irregularly in a meteorite powder because of the difficulty in milling metallic Fe. Other minerals carrying Fe are the silicates olivine and pyroxene, and the iron sulfide troilite. During terrestrial weathering, metallic iron is replaced by iron oxides and iron hydroxides. The latter typically forms a dense network of veins. Where such veins reach the surface of the meteorite and form iron-rich patches, this may yield increased Fe concentrations when measuring with HHXRF. One has to be aware that the measuring depth of Fe is <1 mm, and because iron is a dense element, it could cause shielding.

Cobalt

Cobalt concentrations in chondritic meteorites are in the range of 300–1000 p.p.m., just above the instrument's LOD. This results in large error bars (Fig. 5(g)). However, the content of Co is not critical for chondrite classification, as it would be for iron meteorites, but is important to discriminate from artificial or terrestrial materials. The quantification of Co at high Fe concentrations, as is common in meteorites, is difficult because of an overlap of *Kα* line of Co with the *Kβ* line of Fe.

Nickel

Nickel concentrations range from 50 p.p.m. up to 2 wt% in the tested meteorites (Fig. 5(h)). Most meteorites have Ni contents of about 1.1%. The most important nickel-bearing mineral is taenite, native iron nickel. During weathering of chondritic meteorites, Fe–Ni metal is preferentially weathered, and some Ni are lost.[34,42] On meteorite surfaces in direct contact with soil, often, a pale green mineral is observed that was identified as Ni-serpentine.[34] HHXRF measurements on buried surface of weathered meteorites often show an enrichment of Ni. Some of Ni remains within the meteorite in the form of iron hydroxides.[42]

Strontium

Freshly fallen chondritic meteorites have strontium concentrations of ~10 p.p.m. Weathering and contamination in hot deserts can lead to Sr increases by a factor 10 to 1000.[34] HHXRF provides reliable Sr data over the whole concentration range from fresh to weathered samples (Fig. 5(i)). The results from the experiments for signal depths of contaminants indicate that Sr can be traced up to 2 mm within a H chondrite (Fig. 1). The detection of Sr even at low concentrations requires only short measuring times. Mostly, it appears as the first element detected on the screen after 5 to 10 s.

Barium

Unaltered chondritic meteorites have low barium concentrations of about 4 p.p.m.[43] During weathering and contamination in hot deserts Ba can be enriched by a factor of 100.[34] With 300-s measuring time, an LOD of about ~100 p.p.m. was found for Ba. In most of the samples, Ba lies below or close to the LOD. However, in case of elevated concentrations and for the spiked pellets, the correlation is good (Fig. 5(j)). Another critical factor in Ba analysis is sample thickness. For samples thinner than 1 cm, it is unlikely to obtain meaningful Ba concentrations because the the instrument was calibrated using samples with a thickness of 1 cm. Barium is the only element of interest, which is measured using the 'high filter' of the instrument. If Ba is not required, the 'high filter' can be switched off, saving 120 s of measuring time with the settings used here. With the current instrument, low Ba contaminations (4–100 p.p.m.) are thus not detectable.

Other elements

The concentrations of all other elements measurable with HHXRF mostly are below the LOD in fresh and weathered meteorites. Elements at the LOD are S, V, Zn, As, Zr, Nb, Mo and Pb. In some cases, they fit well to the standard value, but often, they are overestimated, especially S, V, As and Nb because these elements are difficult to measure with a PIN detector at the concentration they appear in meteorites. Because of the lower precisions and accuracies and their limited importance for meteoritics, these elements were not investigated systematically.

Applications of handheld X-ray fluorescence in meteoritics

We have tested several applications in the field of meteorite analysis where HHXRF proved to be a powerful tool. Some of these take advantage of its portability and are thus specifically field-related applications, whereas others profit from its simple handling and the possibility of the fast collection of large amounts of geochemical data in the laboratory for statistical studies.

Identification of doubtful meteorites

During the search for meteorites, often, materials of unidentified nature are encountered. Because most of the common meteorites contain metallic iron, a test with a magnet or a susceptibility meter can help in their recognition. However, several rare types of meteorites are not ferromagnetic and have a low susceptibility and may be missed. With a short HHXRF measurement, it is possible to unequivocally identify most types of meteoritic materials and distinguish them from terrestrial rocks and man-made artifacts. Magnetic meteorites typically have Ni contens >1 wt%, and nonmagnetic meteorites (e.g. lunar or martian rocks) have characteristic element ratios (particularly Fe/Mn) distinguishable from terrestrial rocks. In addition to magnetic susceptibility measurements for the identification of meteorites (e.g. see Folco *et al.*,[44]), HHXRF is an instrument that allows the rapid identification of most types of meteorites in the field. As an example, we did identify meteorite Ramlat as Sahmah (RaS) 287 as diogenite (orthopyroxenite probably derived from asteroid Vesta) while still in the finding position in January 2009. This classification was later confirmed by mineralogical and oxygen isotopic analyses.

During terrestrial residence, meteorites often break up into several rusty fragments.[34] In hot deserts environments, such small fragments are easily recognized but, in some cases, cannot be discriminated from bits of corroded cans and other human waste, or terrestrial Fe-hydroxide nodules and magnetite pebbles. In such cases, a short HHXRF measurement provides a reliable answer on the basis of Ni concentration. Similarly, HHXRF was used in the prospection for fragments of the Twannberg meteorite[45] near Twann, Switzerland. Meteoritic fragments can easily be detected among large numbers of magnetic fragments extracted from a small stream, on the basis of the presence of Fe and Ni and the absence of Cr (present in Ni–Cr steels).

Fast classification of meteorites

Although most chondrites have very similar compositions, they are distinguishable in terms of bulk chemistry, mainly by variations in Ca, Mn, Fe and Ni. The most robust method was found to be a plot of bulk Fe *versus* bulk Mn or bulk Ni *versus* Fe/Mn ratio (Fig. 6). Fields in Fig. 6 show the ranges of published compositional data for falls (achondrites and chondrites; Mittlefehldt *et al.*,[31] and the references therein, Mittlefehldt[46] and the references therein, Jarosewich,[37] Wasson and Kallemeyn,[43] Mason[47] and Kallemeyn *et al.*,[48]) and finds (achondrites,[31] references therein,[46] references therein, Actlab) for the most important and common meteorite classes. Ordinary chondrites are divided into LL, L and H chondrites based on the metal content and the degree of oxidation of Fe-Mg silicates i.e. H chondrites have higher bulk Fe and Ni contents and lower Mn contents and more Mn-rich olivines and pyroxenes. That the limit between LL and L chondrites is not sharp is what makes it difficult for HHXRF analyses. Additionally, terrestrial weathering changes the bulk composition. Loss of Ni, S and, to some extend, Co is observed in strongly weathered meteorites recovered from Oman.[34] Iron is also mobilized during weathering and forms a dense network of Fe-oxide/hydroxide veins inside the meteorite and is also accumulated in the weathering rind in the outer parts of meteorites.[42] Measurements by HHXRF on natural surfaces (NSs) can thus result in overestimated bulk Fe contents while inside the meteorite; on CSs, it is underestimated, resulting in lower Fe/Mn ratios as observed in Fig. 6.

The approximate classification of achondrites often is possible by visual inspection. Achondrites are meteorites with igneous

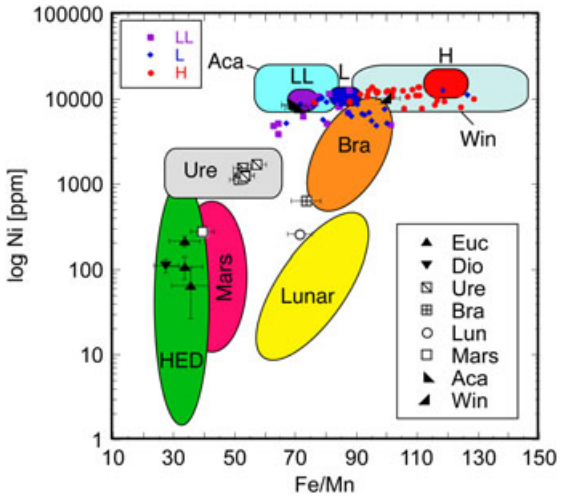

Figure 6. Classification diagram for meteorites using bulk elemental data obtained by handheld X-ray fluorescence. Fields show the ranges of published compositional data for falls and finds for the most important and common meteorite classes. Symbols represent 300-s HHXRF measurements obtained on cut surfaces of meteorite finds, mainly from the Sultanate of Oman. The displayed fields for the ordinary chondrites (LL, L and H) only include data from falls. Weathering effects lower the Ni content.[34] Acapulcoites (Aca) and winonaites (Win) are primitive achondrites having chondritic bulk chemistry. Ureilites (Ure) and brachinites (Bra) are meteorites with near primitive bulk compositions but igneous textures. Eucrites (Euc) and diogenites (Dio) are differentiated meteorites probably derived from the asteroid 4 Vesta. Lunar (Lun) and martian (Mars) meteorites are also differentiated rocks derived from Earth's Moon and Mars, respectively.

textures and are, in most cases, chemically differentiated. Primitive achondrites (acapulcoites, lodranites and winonaites) have basically chondritic bulk compositions. From these meteorites, only a few bulk chemical data are available and a lot of them are weathered finds resulting in large fields in Fig. 6. Certain types of achondrites are linked to defined parent bodies that have distinct Fe/Mn ratios. For example, lunar meteorites and eucrites (likely derived from asteroid 4 Vesta) can have very similar mineralogies and textures but have distinct Fe/Mn ratios of 60–90 (moon) or 28–35 (eucrites). We have routinely applied HHXRF analyses and derived Fe/Mn ratios for the discrimination of eucrites from lunar meteorites for samples brought to our lab by meteorite collectors. Meteorites probably derived from the differentiated asteroid Vesta 4 (howardites, eucrites and diogenites – summarized as HED) (e.g. see Ruzicka *et al.*,[49]) have basaltic/gabbroid compositions marginally overlapping with the field of martian meteorites. For a more profound classification, in addition to the Ni *versus* Fe/Mn plot, a discrimination of meteorites can be made on the basis of Ca, K or Ti contents.[31]

Combined with visual characteristics, it is possible to classify meteorites by nondestructive HHXRF measurements. However, the best results are obtained on cut meteorite because the effect of terrestrial weathering and contamination is less pronounced than on NSs. In addition, in fusion crusts of meteorites, heavy elements such as Fe, Mn and Ni can be enriched, whereas light elements such as K can be depleted (e.g. see Genge and Grady[50] and Shirai *et al.*,[51]).

For classification, a 60-s measurement with the 'field setup' yields satisfying results. However, a 300-s measurement in 'lab setup' should be used to obtain lower errors and DLs. At least three analyses at three different spots are recommended to obtain a representative result. Studies focused on chemical changes during magmatic differentiation will still have to rely on destructive chemical analyses in future. However, HHXRF is a very suitable tool for the recognition and identification of meteorites.

Weathering effects in soils under meteorites

During oxidation of the Fe–Ni-phases kamacite and taenite, Ni is partially liberated and can be accumulated in the soil under meteorites.[34] Normally, soils in Oman have Ni contents in the range of 20–60 p.p.m. (size fraction $<$0.15 mm), close to LOD of the instrument used. Weathering of meteorites can result in an increase exceeding ten times the pristine value in underlying soils (Fig. 7). Increased Ni contents under meteorites indicate stable position during the terrestrial history of the meteorite, consistent with stable desert surfaces that are required for meteorite accumulation.

Desert varnish

A common feature on terrestrial rocks in hot deserts is a thin black coating called desert varnish (DV). The process of DV formation is not understood in detail, but the main components are identified as clay minerals, often aeolian deposits, Fe–Mn oxides, and organic components related to a suggested involvement of microbes and fungi in DV development (e.g. see Dorn,[52] Garvie *et al.*,[53] and Perry *et al.*,[54]). DVs are Mn-rich and show traces of Ba, Sr and Ti (e.g. see Engel and Sharp[55]). The degree of evolution of a DV can give information on the terrestrial age. Archeologists have applied HHXRF in attempts to date petroglyphs by measurements comparing the DV surfaces with the scratched parts.[56–59] DV is reported on meteorites found in the US,[60] Namibia[61] and Australia[62] with a typical thickness of 70–130 μm, but it can reach 3 mm. By comparing HHXRF data obtained on CSs of meteorites with exposed surfaces (preferably not fusion crusted), the relative enrichment of Mn and other elements is detectable, and the presence of DV's can be inferred. As an example, analyses of the lunar meteorite SaU 169[28] are presented in Fig. 8.

Measuring the degree of Mn enrichment on exposed surfaces can be used as proxy of the terrestrial history of the meteorite. A strong enrichment on averagely to heavily weathered samples indicates a stable position on the soil implying the presence of an

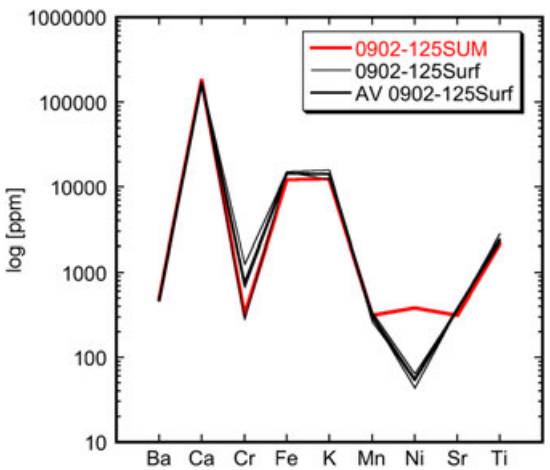

Figure 7. Handheld X-ray fluorescence measurements of soil samples from the find site of meteorite RaS 316 (field No. 0902–125) in Oman. Sample SUM refers to 'soil under meteorite' and shows a strong enrichment of Ni as compared with measurements of reference soil samples from the surface (Surf).

area ideal for the accumulation of meteorites over long periods. Potassium, lead and titanium that are enriched in the DV could also be taken into account but are difficult to measure at the expected concentrations because of high LOD and low precision. The development of DV on meteorites likely is correlated with terrestrial age but is also influenced by soil stability and sand-blasting. We explore the suitability of regional DV abundance on meteorites as an indicator of surface stability and meteorite preservation potential.

Approximative terrestrial age dating based on Ba and Sr accumulation

For an estimation of the terrestrial residence time of a meteorite, a number of parameters that change after arrival on Earth can be measured (degree of oxidation and water content). They are the results of interaction of meteorites with the terrestrial environment. Oxidative weathering and contamination from the soil are important factors.

In this context, our main application of HHXRF is to analyze natural and CSs of meteorites from the Sultanate of Oman to study the effects of terrestrial contamination. The aim was to correlate the Sr and Ba enrichment in ordinary chondrites with the terrestrial age obtained by radiocarbon dating (e.g. see Jull[63]) to establish an approximative age scale. In the Oman case, Sr and Ba concentrations are independent indicators of a meteorite's terrestrial age. This allows the designation of a crude terrestrial age to each sample collected. The comparison of the large number of approximate ages with the smaller number of ^{14}C-dated samples provides a control to check for a bias in the samples selected for ^{14}C dating.

Pairing issues and recognition of find areas

In recent years, large amounts of meteorites have been recovered in hot deserts, especially in NWA (defined by the Meteoritical Society as 'Morocco and parts of adjoining neighboring countries'). Because of the unknown find conditions, NWA meteorites may also include samples from other countries such as Mali, Niger, Libya and even Oman. By far, the largest number is from 'NWA' and lacks geographical information. Many meteorites, especially the ordinary chondrites, are not properly classified because this is time consuming and the scientific and commercial interest is mainly focused on achondrites and rare types of chondrites. Meteorites usually break up in the atmosphere, and several fragments reach the Earth, forming strewn fields (e.g. see Clarke *et al.*,[29] and Gnos *et al.*,[64]). A short measurement by HHXRF provides a fast first classification, which helps to recognize pairing groups (i.e. meteorites from the same fall event). The recognition of pairings is important for the determination of absolute fall abundances and statistical studies of the global meteorite influx derived from such data. Criteria applied include bulk compositional data (Fe/Mn, Ni, Cr and Ca) and the amount of terrestrial contamination (Ba, Sr and Mn) on NSs'.

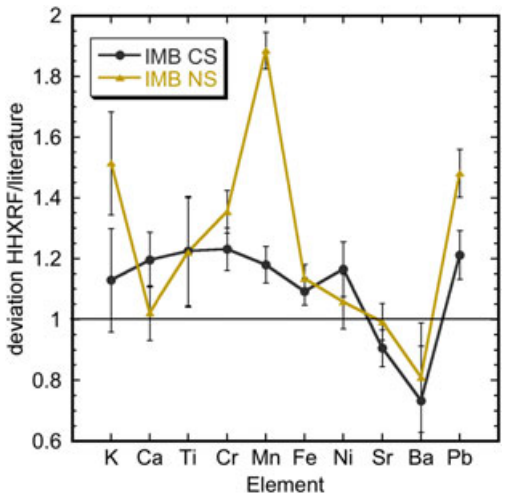

Figure 8. Handheld X-ray fluorescence (HHXRF) measurements of the impact melt breccia (IMB) portion of the lunar meteorite SaU 169 normalized to literature values of homogenized bulk samples.[28] Taking into account the slightly different matrix of this sample as compared with the meteorites used for calibration, the HHXRF measurements are in good agreement with published values except for significantly elevated values of Mn, K and Pb on the natural surface (NS), indicating the development of a thin desert varnish enriched in these elements. Each data point represents the median of 4 to 11 measurements of 300 s. CS, cut surface.

Conclusions

The newly developed commercial HHXRF analyzers are powerful tools for simple and fast collection of element concentration data from meteorites and associated terrestrial materials. Because the method is nondestructive it is very helpful for the study of precious materials such as meteorites.

No sample preparation is needed, but because the measurement spot is 8 mm in diameter, at least three measurements are recommended to get reliable results. The calibration curves of our HHXRF device were slightly adjusted for meteorite and desert soil matrices. Deviations between 10% and 20% from standard values are reached for most important elements. The instrument is useful for the identification of doubtful meteorites in the field and for the chemical classification of the most abundant groups of chondrites and achondrites. Terrestrial contamination effects such as the accumulation of Ba, Sr and Mn or the loss of Ni are easily traceable with a 300-s HHXRF measurement. A combination of these two applications can help in solving pairing issues. Because of the speed, easy handling and nondestructive character of analysis, the instrument is a useful tool in meteoritics both in the field and in the laboratory.

The latest generation of HHXRF instruments equipped with SDD will yield much more precise analyses on more elements with lower LOD because they have a better energy resolution, which produces a better peak-to-background ratio.

Acknowledgements

We thank Stan Piorek, Marc Dupayrat, Roland Bächli and Björn Klaue for the support in adapting the Niton instrument and constructive comments on the initial version of the manuscript. Salim Omar Al-Ibrahim, Director General of Minerals, is thanked for the permission to carry out meteorite research in the Sultanate of Oman. We would like to appreciate the help of Nicolas Greber during meteorite analyses. Marc Jost is acknowledged for preparation of thin meteorite slices for the shielding experiments. We thank the three anonymous reviewers for their suggestions to improve the manuscript and René Van Grieken for editorial handling. This study was supported by the Swiss National Science Foundation (SNF), grant 200020–119937.

References

[1] S. J. B. Reed, *Meteoritics* **1972**, *7*, 257.
[2] S. J. Goldstein, A. K. Slemmons, H. E. Canavan, *Environ. Sci. Technol.* **1996**, *30*, 2318.
[3] T. Radu, D. Diamond, *J. Hazard. Mater.* **2009**, *171*, 1168.
[4] C. Roldan, S. Murcia-Mascaros, J. Ferrero, V. Villaverde, E. Lopez, I. Domingo, R. Martinez, P. M. Guillem, *X-Ray Spectrometry* **2009**, *39*, 243.
[5] Z. Szokefalvi-Nagy, I. Demeter, A. Kocsonya, I. Kovacs, *Nucl. Instrum. Methods Phys. Res., Sect. B* **2004**, *226*, 53.
[6] L. Bonizzoni, S. Caglio, A. Galli, G. Poldi, *X-Ray Spectrometry* **2010**, *39*, 233.
[7] X. Hou, Y. He, B. T. Jones, *Appl. Spectrosc. Reviews* **2004**, *39*, 1.
[8] A. E. Rubin, J. N. Grossman, *Meteoritics & Planetary Sci.* **2010**, *45*, 114.
[9] O. R. Norton, L. A. Chitwood, *Field Guide to Meteors and Meteorites*, Patrick Moore's Practical Astronomy Series, Springer, London, **2008**.
[10] R. Harvey, *Chemie Der Erde—Geochemistry* **2003**, *63*, 93.
[11] A. W. R. Bevan, R. A. Binns, *Meteoritics* **1989**, *24*, 127.
[12] A. W. R. Bevan, R. A. Binns, *Meteoritics* **1989**, *24*, 135.
[13] A. J. T. Jull, L. R. McHargue, P. A. Bland, R. C. Greenwood, A. W. R. Bevan, K. J. Kim, S. E. LaMotta, J. A. Johnson, *Meteoritics & Planetary Sci.* **2010**, *45*, 1271.
[14] J. Otto, *Chemie der Erde* **1992**, *52*, 33.
[15] A. Bischoff, T. Geiger, *Meteoritics* **1995**, *30*, 113.
[16] J. Schlüter, L. Schultz, F. Thiedig, B. O. Al-Mahdi, A. E. Abu Aghreb, *Meteoritics & Planetary Sci.* **2002**, *37*, 1079.
[17] N. L. Ouazaa, N. Perchiazzi, S. Kassaa, A. Zeoli, M. Ghanmi, L. Folco, *Meteoritics & Planetary Sci.* **2009**, *44*, 955
[18] A. Al-Kathiri, PhD thesis, University of Bern (Bern), **2006**.
[19] D. C. Hezel, J. Schlüter, H. Kallweit, A. J. T. Jull, O. Y. Al-Fakeer, M. Al-Shamsi, S. Strekopytov, *Meteoritics & Planetary Science* **2011**, *46*, 327.
[20] C. Munoz, N. Guerra, J. Martinez-Frias, R. Lunar, J. Cerda, *J. Arid Environ.* **2007**, *71*, 188.
[21] M. E. Zolensky, G. L. Wells, H. M. Rendell, *Meteoritics* **1990**, *25*, 11.
[22] A. J. T. Jull, D. J. Donahue, E. Cielaszyk, F. Wlotzka, *Meteoritics* **1993**, *28*, 188.
[23] P. Rochette, L. Sagnotti, M. Bourot-Denise, G. Consolmagno, L. Folco, J. Gattacceca, M. L. Osete, L. Pesonen, *Meteoritics & Planetary Sci.* **2003**, *38*, 251.
[24] P. Rochette, J. Gattacceca, M. Bourot-Denise, G. Consolmagno, L. Folco, T. Kohout, L. Pesonen, L. Sagnotti, *Meteoritics & Planetary Sc.* **2009**, *44*, 405.
[25] P. Rochette, J. Gattacceca, L. Bonal, M. Bourot-Denise, V. Chevrier, J. P. Clerc, G. Consolmagno, L. Folco, M. Gounelle, T. Kohout, L. Pesonen, E. Quirico, L. Sagnotti, A. Skripnik, *Meteoritics & Planetary Sci.* **2008**, *43*, 959.
[26] NITON, *User's Guide* **2008**, 202.
[27] E. Gnos, B. Hofmann, I. A. Franchi, A. Al-Kathiri, M. Hauser, L. Moser, *Meteoritics & Planetary Sci.* **2002**, *37*, 835.
[28] E. Gnos, B. A. Hofmann, A. Al-Kathiri, S. Lorenzetti, O. Eugster, M. J. Whitehouse, I. M. Villa, A. J. T. Jull, J. Eikenberg, B. Spettel, U. Krahenbuhl, I. A. Franchi, R. C. Greenwood, *Science* **2004**, *305*, 657.
[29] J. Clarke, S. Roy, E. Jarosewich, B. Mason, J. Nelen, M. Gomez, J. R. Hyde, *Smithson. Contrib. Earth Sci.* **1971**, 5.
[30] E. Jarosewich, J. Roy S. Clarke, J. N. Barrows, *Smithson. Contrib. Earth Sci.* **1987**, 27.
[31] D. W. Mittlefehldt, T. J. McCoy, C. A. Goodrich, A. Kracher, In *In Planetary Materials*, Vol. *36* (Ed.: J. J. Papike), Mineralogical Society of America, Washinton D.C., **1998**, pp. 4.
[32] M. K. Weisberg, T. J. McCoy, Krot A. N., In *Meteorites and the Early Solar System II*, (D. S. Lauretta, (Eds. H. Y. McSween), Univ. Arizona Press, **2006**, 19.
[33] T. Stelzner, K. Heide, A. Bischoff, D. Weber, P. Scherer, L. Schultz, M. Happel, W. Schron, U. Neupert, R. Michel, R. N. Clayton, T. K. Mayeda, G. Bonani, I. Haidas, S. Ivy-Ochs, M. Suter, *Meteoritics & Planetary Sci.* **1999**, *34*, 787.
[34] A. Al-Kathiri, B. A. Hofmann, A. J. T. Jull, E. Gnos, *Meteoritics & Planetary Sci.* **2005**, *40*, 1215.
[35] S. S. Russell, L. Folco, M. M. Grady, M. E. Zolensky, R. Jones, K. Righter, J. Zipfel, J. N. Grossman, *Meteoritics & Planetary Sci.* **2004**, *39*, A215.
[36] E. Gnos, M. Eggimann, A. Al-Kathiri, B. A. Hofmann, *Meteoritics & Planetary Sci.* **2006**, *41 Suppl*, A64.
[37] E. Jarosewich, *Meteoritics* **1990**, *25*, 323.
[38] G. J. Consolmagno, D. T. Britt, R. J. Macke, *Chemie Der Erde-Geochemistry* **2008**, *68*, 1.
[39] H. Y. McSween, M. E. Bennett, E. Jarosewich, *Icarus* **1991**, *90*, 107.
[40] A. E. Rubin, *Meteoritics & Planetary Sci.* **1997**, *32*, 733.
[41] M. Eggimann, PhD thesis, Institut für Geologie (Bern), **2008**.
[42] M. R. Lee, P. A. Bland, *Geochim. Cosmochim. Acta* **2004**, *68*, 893.
[43] J. T. Wasson, G. W. Kallemeyn, *Philos. Trans. R. Soc. Lond. A* **1988**, *325*, 535.
[44] L. Folco, P. Rochette, M. Gattacceca, N. Perchiazzi, *Meteoritics & Planetary Sci.* **2006**, *41*, 343.
[45] B. A. Hofmann, S. Lorenzetti, O. Eugster, U. Krähenbühl, G. Herzog, F. Serefiddin, E. Gnos, M. Eggimann, J. T. Wasson, *Meteoritics & Planetary Sci.* **2009**, *44*, 187.
[46] D. W. Mittlefehldt, In *Treatise on Geochemistry*, Vol. *1* (Ed.: A. M. Davis), Elsevier, **2003**, pp. 711–291.
[47] B. Mason, *American Museum Novitates*, American Museum of Natural history, Central Park West at 79th street, New York, **1962**, *2085*, 429.
[48] G. W. Kallemeyn, A. E. Rubin, D. Wang, J. T. Wasson, *Geochim. Cosmochim. Acta* **1989**, *53*, 2747.
[49] A. Ruzicka, G. A. Snyder, L. A. Taylor, *Meteoritics & Planetary Sci.* **1997**, *32*, 825.
[50] M. J. Genge, M. M. Grady, *Meteoritics & Planetary Sci.* **1999**, *34*, 341.
[51] N. Shirai, M. Humayun, A. J. Irving, in *40th Lunar and Planetary Science Conference*, **2009**, p. 2170.
[52] R. I. Dorn, *Geography Compass* **2009**, *3*, 1.
[53] L. A. J. Garvie, D. M. Burt, P. R. Buseck, *Geology* **2008**, *36*, 215.
[54] R. S. Perry, B. Y. Lynne, M. A. Sephton, V. M. Kolb, C. C. Perry, J. T. Staley, *Geology* **2006**, *34*, 537.
[55] C. G. Engel, R. P. Sharp, *Geol. Soc. Am. Bull.* **1958**, *69*, 487.
[56] F. Lytle, Nevada Rock Art Foundation meeting, *Mesquite NV* **2009**.
[57] N. E. Pingitore, F. W. Lytle, P. D. Rowley, D. E. Ferris, American Geophysical Union, Fall Meeting 2004, **2004**, abstrct #B33B.
[58] N. E. Pingitore, F. W. Lytle, *EOS Trans. AGU* **2003**, 84.
[59] F. W. Lytle, N. E. Pingitore, N. W. Lytle, D. Ferris-Rowley, M. C. Reheis, Workshop on Synchrotron Radiation in Art and Archaeology, SSRL **2000**.
[60] D. A. Kring, A. J. T. Jull, L. R. McHargue, P. A. Bland, D. H. Hill, F. J. Berry, *Meteoritics & Planetary Sci.* **2001**, *36*, 1057.
[61] R. F. Fudali, A. F. Noonan, *Meteoritics* **1975**, *10*, 31.
[62] M. R. Lee, P. A. Bland, *Earth Planet. Sci. Lett.* **2003**, *206*, 187.
[63] A. J. T. Jull, *Terrestrial ages of meteorites*, The University of Arizona Press, Tucson, AZ, **2006**.
[64] E. Gnos, S. Lorenzetti, O. Eugster, A. J. T. Jull, B. A. Hofmann, A. Al-Kathiri, M. Eggimann, *Meteoritics & Planetary Sci.* **2009**, *44*, 375.

